

Noncovalent Bonding Controls Selectivity in Heterogeneous Catalysis: Coupling Reactions on Gold

Stavros Karakalos,^{†,||} Yunfei Xu,[†] Fairoja Cheenicode Kabeer,[‡] Wei Chen,^{§,⊥,∇} Juan Carlos F. Rodríguez-Reyes,[○] Alexandre Tkatchenko,^{‡,#} Efthimios Kaxiras,^{†,§,⊥} Robert J. Madix,[§] and Cynthia M. Friend^{*,†,§}

[†]Department of Chemistry and Chemical Biology, [§]Harvard John A. Paulson School of Engineering and Applied Sciences, and [⊥]Department of Physics, Harvard University, Cambridge, Massachusetts 02138, United States

[‡]Fritz-Haber-Institut der Max-Planck-Gesellschaft, Faradayweg 4-6, Berlin D-14195, Germany

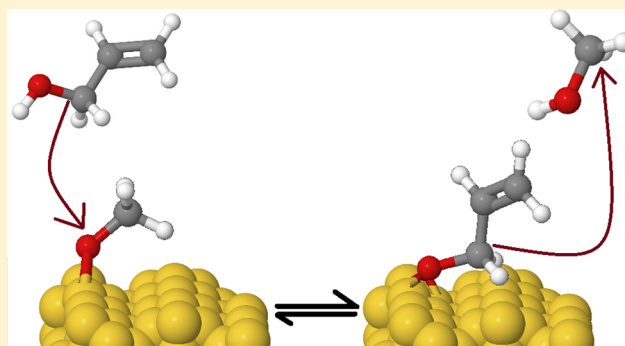
[∇]ICQD, Hefei National Laboratory for Physical Sciences at Microscale, and Synergetic Innovation Center of Quantum Information and Quantum Physics, University of Science and Technology of China, Hefei, Anhui 230026, China

[○]Department of Industrial Chemical Engineering, Universidad de Ingeniería y Tecnología, Avenida Cascanueces 2221, Lima 43 15063, Peru

[#]Physics and Materials Science Research Unit, University of Luxembourg, Luxembourg City L-1511 Luxembourg

Supporting Information

ABSTRACT: Enhancing the selectivity of catalytic processes has potential for substantially increasing the sustainability of chemical production. Herein, we establish relationships between reaction selectivity and molecular structure for a homologous series of key intermediates for oxidative coupling of alcohols on gold using a combination of experiment and theory. We establish a scale of binding for molecules with different alkyl structures and chain lengths and thereby demonstrate the critical nature of noncovalent van der Waals interactions in determining the selectivity by modulating the stability of key reaction intermediates bound to the surface. The binding hierarchy is the same for Au(111) and Au(110), which demonstrates a relative lack of sensitivity to the surface structure. The hierarchy of binding established in this work provides guiding principles for predicting how molecular structure affects the competition for binding sites more broadly. Besides the nature of the primary surface-molecule bonding, three additional factors that affect the stabilities of the reactive intermediates are clearly established: (1) the number of C atoms in the alkyl chain, (2) the presence of C–C bond unsaturation, and (3) the degree of branching of the alkyl group of the adsorbed molecules. We suggest that this is a fundamental principle that is generally applicable to a broad range of reactions on metal catalysts.



INTRODUCTION

Achieving high selectivity for chemical transformations is a central goal in catalysis because of the potential for enhancing the efficiency and sustainability of chemical synthesis. Selective oxidation reactions, in particular, are of interest because of their widespread use in large-scale chemical production. Consequently, there is great interest in the development of principles for optimizing activity and product selectivity in heterogeneous catalysis in general and for selective oxidation processes specifically.

Accordingly, there has been a drive to parametrize surface reactivity using critically important factors, such as adsorbate binding energy, as a means of predicting and screening effective materials for specific reactions, such as ammonia synthesis. Considerable progress has been made in understanding periodic trends among transition-metal catalysts for various

reactions through the use of scaling relationships based on metal-atom bond strengths (C, O, N) and reactivity.^{1–4} In more complex reaction environments, however, more subtle factors, such as secondary interactions of intermediates with the surface, may play a role. If the effect of molecular structure differs across the periodic table, vdW interactions may tip the balance sufficiently to cause significant deviation from the behavior suggested by this metal-atom bonding scaling approach.

A key factor in determining the catalytic performance in complex reaction environments is competition for reactive sites among reactants and reaction intermediates on the catalyst surface.⁵ In fact, reactants with analogous structures can

Received: September 8, 2016

Published: October 24, 2016

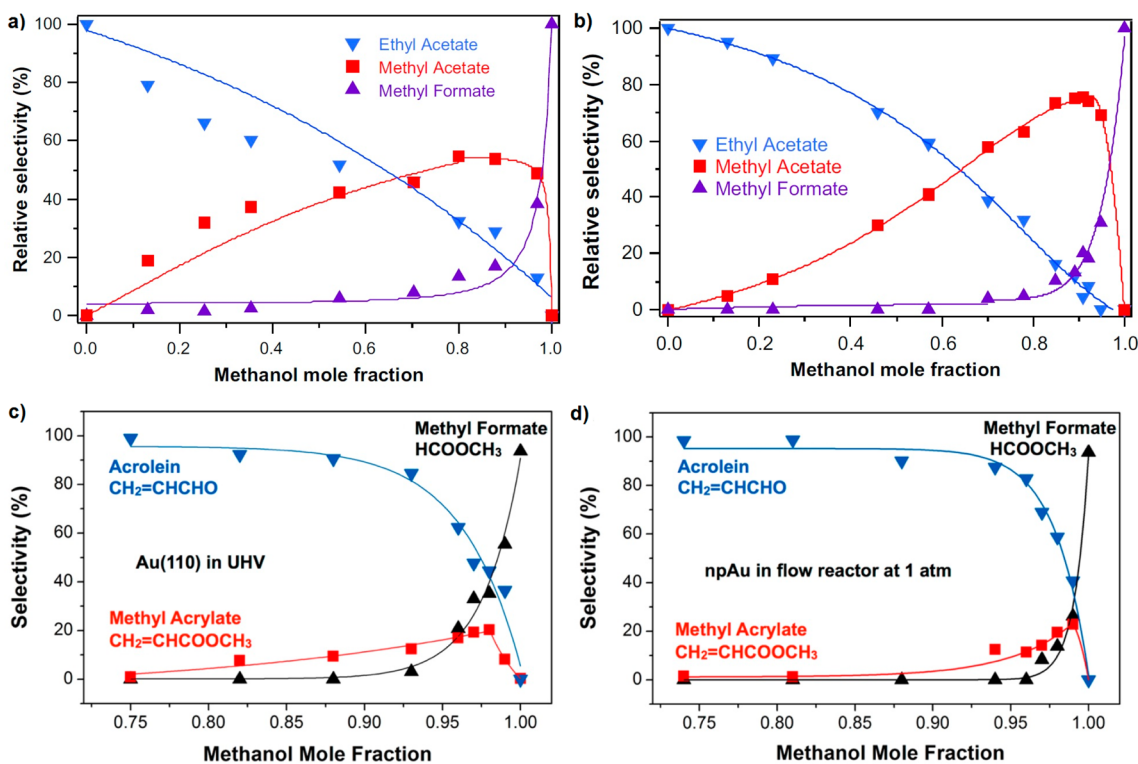


Figure 1. The selectivity of methanol coupling with ethanol (top) and allyl alcohol (bottom). The dependence on the methanol mole fraction is very similar on Au single crystals and on a nanoporous Au catalyst. Coupling of methanol and ethanol (a) on Au(111) and (b) on npAu.¹⁰ Coupling of methanol and allyl alcohol (c) on Au(110) and (d) on npAu.¹¹ The optimum cross coupling selectivity occurs when the molar fraction of methanol is higher than 0.85 in the case of cross-coupling with ethanol and higher than 0.95 in the case of allyl alcohol, illustrating the competitive binding of the dissimilar alkoxides on Au catalysts. Figure adapted with permission from refs 10 and 11.

compete via displacement reactions between species in the ambient phase and the adsorbed reactive intermediate.^{6,7} This competition for active sites can be dramatically affected by small differences between the binding energies of the competing intermediates to the surface, due to the exponential dependence of the equilibrium constants of this displacement reaction on the relative binding energy of the species to the surface.


The work described herein is motivated by previous studies under catalytic conditions that illustrate the effect of competitive binding in the selectivity for the oxygen-assisted cross-coupling of methanol with a second dissimilar, short-chain alcohol^{7–9} to form methyl esters on metallic gold-based catalysts (Figure 1).^{10,11} To a good approximation, the optimum cross coupling occurs when the surface concentration of the two different alkoxy intermediates is equal, as the cross-coupling originates from the surface reaction between the dissimilar alkoxy species. If the O–Au bond strength dictates the binding energy, methoxy and ethoxy,² for example, would have nearly identical surface stabilities. Thus, equal surface concentrations of methoxy and ethoxy would be expected for a 50–50 composition in the reactant mixture. Contrary to this prediction, a much higher molar fraction of methanol (>0.85) is required in the reactant mixture to maximize formation of methyl acetate.⁶ Previously, we showed that inclusion of van der Waals (vdW) interactions qualitatively predicts that ethoxide is more strongly bound to Au(111) than methoxide.⁵ The importance of these weak interactions under catalytic conditions is demonstrated by the fact that the selectivity for ester formation vs methanol mole fraction is essentially the

same under catalytic flow conditions using nanoporous Au and on Au(111).

Evaluation of the effect of C=C bonds on binding efficacy is an important factor based on experimental studies of competitive binding of methanol and alkoxides with C=C bonds. For example, in the case of methanol coupling with allyl alcohol to form methyl acrylate, an even larger excess of methanol is required (>0.95) to achieve optimum selectivity both for model studies on Au(110) and under catalytic flow conditions using nanoporous Au (Figure 1). We attribute this unusual dependence of selectivity on the reactant mixture composition to the stronger, and hence preferential, binding of alkoxy species with longer alkyl chains, alkyl branching or with C=C bonds relative to methoxy. In this work, we set out to test this hypothesis.

The work described herein provides several new insights into factors that control competitive binding of key intermediates under reaction conditions, including demonstration of the enhanced binding due to noncovalent interactions of C=C bonds in the alkoxides and of the relative lack of surface sensitivity on binding of alkoxides with a range of molecular structures by comparison of Au(111) and Au(110). Furthermore, a well-defined and uniform scale of relative binding is established by referencing all theoretical calculations to water formation from acid–base reactions between adsorbed oxygen and the alcohol, which can be treated as a gas-phase acid. This reference reaction can be broadly used for other gas-phase acids, e.g., amines and carboxylic acids, that produced key intermediates, amides, and carboxylates, through analogous reactions. Thus, this work establishes a scale for evaluating

Table 1. Experimental Hierarchy of Relative Binding on Au(110) and Au(111)^c

Increasing surface stability


CH ₃ O _{ads} Methoxy ^{a,b}	C ₂ H ₅ O _{ads} Ethoxy ^{a,b}	CH ₃ (CH ₂) ₂ O _{ads} 1-Propoxy ^{a,b}	(CH ₃) ₂ CH ₂ O 2-Propoxy ^b	H ₂ C=CHCH ₂ O _{ads} Alloxy ^b	H ₂ C=CHC(H)(CH ₃)O _{ads} Methallyloxy ^b	C ₆ H ₅ -CH ₂ -O _{ads} Benzyloxy ^{a,b}
--	---	--	---	--	--	--

^aExperiments performed on Au(111). ^bExperiments performed on Au(110) (Figure S2 and S3). ^cOrdered stabilities of surface intermediates of their parent acid (BH), signature reaction products used to identify each alkoxy reaction intermediate and its characteristic temperature.

relative binding not only on Au but also on other transition metals.

METHODS

Experimental Section. All experiments were performed under ultrahigh vacuum conditions in a chamber with a base pressure of $\sim 1 \times 10^{-10}$ Torr. The chamber was outfitted with a mass spectrometer (Hiden, HAL301) for the detection of products of temperature-programmed reaction, Auger electron spectroscopy (AES) to verify the cleanliness of the surface and low-energy electron diffraction (LEED) for determining the surface order. The Au crystals were mounted on a manipulator capable of heating to 1000 K and of cooling (via liquid nitrogen) to 100 K, as measured by a chromel–alumel thermocouple inserted into a pinhole in the side of the crystals. The surface structure was confirmed to be the characteristic Au(110)-(2 × 1) reconstruction using LEED.

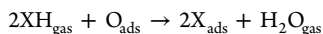
Gold single crystals were cleaned by argon ion bombardment followed by cycles of ozone dosing at 200 K and flash annealing to 850 K to remove surface impurities (as judged by CO and CO₂ production from C contaminations). Surface cleanliness was also confirmed by ordered LEED patterns.

Experiments were performed on both Au(110) and Au(111) surfaces covered with 0.05 ML atomic oxygen. Atomic oxygen was generated by introducing ozone to the surface.^{6,12} Ozone was produced using a commercial ozone generator (Ozone Engineering, LG-7) fed by an O₂ flow, generating a mixture of $\sim 10\%$ O₃ in O₂ which was then introduced to the surface using a directed doser. The coverage of adsorbed O was calibrated by comparison of the integrated O₂ signal due to O atomic recombination above 500 K to the integrated signal for the saturation coverage of 1 ML.¹³

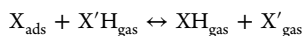
The purities of the organic compounds employed were established after freeze–pump–thaw cycles by measuring the fragmentation patterns obtained from sublimation after condensation at 120 K. In all cases, the fragmentation patterns were in good agreement with those reported in the NIST database. Furthermore, we found that the traces for all fragments could be superimposed after scaling, indicative of the purity of the compound.

General procedures for temperature-programmed reaction spectroscopy (TPRS) have been described previously.^{14,15} The heating rate was constant at 5 K/s in all cases. Our experimental design included the collection of traces in the range $m/z = 2$ to $m/z = 2m$, where m is the molecular mass of the heaviest compound. Extensive calibrations and careful control of conditions (Figure S1) were used to ensure that reproducible doses of the species were delivered to the surface.⁵

Theory. The basic reaction considered for the calculation of the adsorption energy is the organic molecule XH selectively reacts with O bound to the gold surface according to



The hierarchy of surface stabilities of the intermediate X_{ads} is established by investigating the displacement reaction⁵ on the gold surface:



We used the DFT codes FHI-aims¹⁶ and VASP¹⁷ to investigate the stability hierarchy of adsorbates on the Au(111) and Au(110) surfaces, respectively. The two codes were shown to agree very well in a recent

benchmark study.¹⁸ We have further established that the two codes are in excellent agreement as employed here by benchmark studies of methoxy adsorbed on Au(111) (see Supporting Information). We used the DFT+vdW^{surf} method^{19,20} in both codes to account for the vdW correction. This method combines the Tkatchenko–Scheffler (TS) DFT+vdW¹⁹ method for intermolecular interactions with the Lifshitz–Zaremba–Kohn (LZK) theory^{21,19} and therefore goes beyond the pairwise approximation by including the collective response of the substrate electrons in the calculation of adsorbate–substrate vdW interactions.

We employed the “tight” settings for the integration grids and standard numerical atom-centered orbitals basis sets in the FHI-aims code,¹⁶ which is an all-electron full potential electronic structure code. The atomic zeroth-order regular approximation (ZORA)²² was used to treat the relativistic effects for all atoms. A 5 × 5 surface cell with 6 metal layers, consisting of 150 Au atoms, was used to represent the experimental conditions of low oxygen coverage on Au surfaces. The uppermost two layers were allowed to fully relax with the adsorbed molecule during the geometry relaxation, whereas the bottom four layers were fixed at their bulk positions. The three lattice vectors of each slab were 14.72, 14.72, and 60.00 Å, respectively, with a vacuum region of more than 40 Å in the z direction. The FHI-aims code uses atomic basis sets allowing the large vacuum without dramatically increasing computation time. We used a 3 × 3 × 1 k -point mesh for the surface calculations.

For calculations on Au(110) surface, we used the projector-augmented wave (PAW) potentials²³ in VASP,¹⁷ which is a plane-wave code. We employed the GGA-PBE²⁴ for the exchange–correlation functional and the PBE+vdW^{surf} method for vdW-inclusive calculations. The energy cutoff was 400 eV for the plane-wave basis sets. We employed the Au(110)-(1 × 2) surface with a missing row reconstruction for calculations. The Au(110) surfaces were modeled by slabs of five atomic layers, each slab consisting of 72 Au atoms. During structural optimization, Au atoms in the lower two atomic layers were fixed in their bulk positions, and all the other atoms were allowed to relax. The three lattice vectors of each slab were 16.62, 11.75, and 22.24 Å, respectively, with a vacuum region of more than 12 Å in the z direction, to ensure decoupling between neighboring slabs. For the Au(110) calculations, the size of the vacuum was tested, and converged results were obtained at 12 Å. A 4 × 5 × 1 k -point mesh²⁵ was utilized for the 2 × 4 supercell of the Au(110)-(1 × 2) surface.

For all calculations, the initial adsorbed molecular structures were systematically varied by changing their relative position and orientation on the Au(111) and Au(110) surfaces. This allowed a systematic search for the most stable structures, which are analyzed in the manuscript.

RESULTS

Here we develop an understanding of how molecular structure, including branching and C–C bond unsaturation, in the bound species affects the relative binding energy of key intermediates that will in turn determine reaction selectivity in coupling reactions. We demonstrate the strong effect of molecular structure, both total and internal, on the binding of alkoxy moieties on Au surfaces. Theoretical studies establish that the inclusion of noncovalent vdW interactions between the

pendant group and the surface is required to account for the hierarchy of binding. This work is a first step in determining whether the effect of these weak interactions may slightly modify the existing scaling relationships if their magnitude varies differently on different transition metals. To illustrate this principle, an experimental hierarchy of the surface binding strength of an extended series of reactive alkoxy intermediates is established on both Au(111) and Au(110), and the details of the differences in binding clarified by DFT with vdW interactions.

We establish a qualitative scale of binding experimentally using displacement reactions on single crystal Au(111) and (110) (Table 1).⁵ The equilibrium constant for competition for binding of the methanol–ethanol pair has also been determined on both surfaces to provide a more quantitative measure of the competition (Figure 2). The displacement reactions are

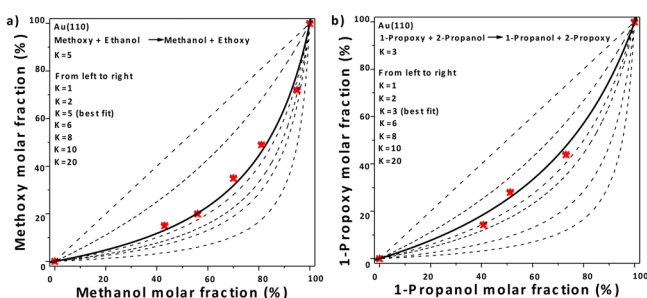


Figure 2. Equilibrium constant measurements between methanol/ethanol and 1-propanol/2-propanol on Au(110). The fraction of surface (a) methoxy and (b) 1-propoxy are plotted as a function of methanol and (b) 1-propanol molar fractions in the alcohol mixtures. The points are the data analyzed from experiment. The various dashed lines represent the surface concentrations of the alkoxy species as a function of methanol or 1-propanol molar fractions, for different equilibrium constants between the reactant mixtures and the surface alkoxy species.

performed at very low total coverage so as to minimize possible intermolecular interactions. The total coverage of alkoxy species is determined by the starting concentration of atomic O on the surface since O_{ads} is required for initial formation of the alkoxy; i.e., O_{ads} is the active site for reaction.⁷ The adsorbed oxygen is quantitatively removed as water. Since no reaction occurs on clean Au surfaces, isolated adsorbed alkoxy species can be created and isolated by reacting alcohols with Au(111) or Au(110) surfaces containing 0.05 ML of preadsorbed O at 120 K, followed by heating to 190 K. Subsequent exposure of the isolated alkoxy to an excess of another alcohol can lead to displacement of the preformed alkoxy if the bonding of the alkoxy associated with the incoming alcohol is stronger. The relative binding efficacy of the various alkoxy species reflects thermodynamic stability and not kinetic limitations based on the fact that the hierarchy was the same, independent of the order of adsorption. Thus, possible changes in the activation energy for displacement are not a factor in the determination of the binding hierarchy. In all cases, a signature product resulting from the temperature-programmed reaction of the specific isolated alkoxy species was used to determine which intermediate was present on the surface (Table ST1 and Figures S2 and S3).

The hierarchy of binding determined experimentally (Table 1) demonstrates that several factors affect the intermediate's surface stability, namely, (1) the number of carbon atoms in the chain, (2) the presence of carbon–carbon bond unsaturation,

and (3) the branching configuration of the hydrocarbon chain. For the straight chain alkoxy species, the binding energy to the surface increases with chain length on both Au(110) and Au(111). The effect of chain branching is demonstrated by the displacement of 1-propoxy by 2-propanol (Figure S2A). The stabilization effect of C=C bond unsaturation is shown by the displacement of 2-propoxy by allyl alcohol on Au(110) (Figure S2B). Further methallyloxy displaces allyloxy,¹¹ showing that even the addition of a single methyl group to the unsaturated alkoxy results in increased stabilization of the surface intermediate. Further, benzyl alkoxy displaces methallyloxy (Figure S2C); the aromatic ring results in stronger attractive interactions with the substrate than the C=C unsaturated bond (see Figures S2 and S3). The order of stability for alkoxy intermediates is identical on both Au(111) and Au(110), demonstrating the absence of structure sensitivity on the displacement.

A more quantitative evaluation of the relative binding efficacy for different alkoxy species is the equilibrium constants for competitive binding of mixtures of alcohols on the surfaces. The equilibrium constant for displacement of methoxy by ethanol is measured as 5 ± 1 at 200 K (essentially the same as for Au(111)⁶) and for displacement of 1-propoxy by 2-propanol is measured as 3 ± 1 at 200 K on Au(110). The equilibrium constants for the methanol/ethanol and 1-propoxy/2-propanol competition demonstrate that ethoxy preferentially binds over methoxy and 2-propanol over 1-propoxy, consistent with the displacement measurements (Table 1). If the alkoxy species in both cases were equally strongly bound, the equilibrium constants would be unity, and the methoxy coverage would vary linearly with methanol molar fraction and the same for 1-propoxy. Deviation from unity is clearly demonstrated by the curvature in the dependence and the fact that the fractional methoxy (1-propoxy) coverage on the surface is smaller than the methanol (1-propanol) molar fraction over the entire mixture composition studied.

Corresponding theoretical calculations of the relative binding energies for various alkoxy species on Au(110) show that inclusion of vdW interactions is required in order to predict the trends in relative binding for alkoxy species with different molecular structure (Table 2).^{26,27} Without inclusion of van der Waals interactions,

Table 2. Effect of vdW Interactions on the Adsorption Energies on Au Surfaces^a

theoretical hierarchy on Au(111) and Au(110)	reaction energy ($-\Delta E$) on Au(111) in eV		reaction energy ($-\Delta E$) on Au(110) in eV	
	PBE	PBE +vdW ^{surf}	PBE	PBE +vdW ^{surf}
benzyl alkoxy	0.20	0.84	0.20	0.92
methallyloxy	0.22	0.73	0.27	0.75
allyloxy	0.22	0.66	0.24	0.68
2-propoxy	0.21	0.59	0.21	0.66
1-propoxy	0.22	0.55	0.22	0.58
ethoxy	0.21	0.44	0.21	0.50
methoxy	0.18	0.28	0.18	0.40

^aCalculated hierarchy of the stability of intermediates on Au(110) and Au(111) obtained with PBE+vdW^{surf} and PBE methods using the reaction: $2\text{XH}_{(\text{g})} + \text{O}_{(\text{ads})} \rightarrow 2\text{X}_{(\text{ads})} + \text{H}_2\text{O}_{(\text{g})}$, to establish a consistent reference for comparison between alkoxy species. The relative values of the reactions energies between alkoxy species are more meaningful than the absolute values (see the Methods section for calculation details).

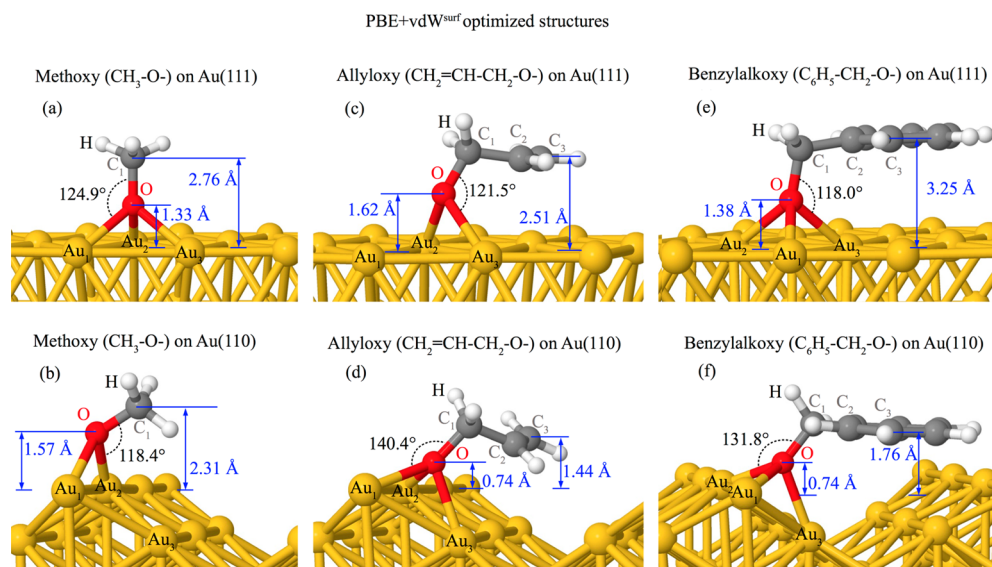


Figure 3. Optimized structures. Methoxy (left), allyloxy (middle), and benzyl alkoxy (right) on the Au(111) (top) and Au(110) (bottom) surfaces determined using PBE+vdW^{surf} calculations. The nearest Au atoms to the adsorbed O atoms (Au₁, Au₂, and Au₃) and several adsorption distances and angles are marked. On the Au(110) surface, Au₁ and Au₂ represent the top row atoms of the missing-row reconstruction. Structures of all the computed adsorbates on both surfaces with or without vdW interactions are shown in Figures S4 and S5.

Table 3. Comparison of Intermediates Adsorbed on Au with and without vdW Interactions^a

systems	O–Au distance Å						C ₃ –Au distance Å		Au–O–C ₁ angle	
	PBE+vdW ^{surf}			PBE			PBE+ vdW ^{surf}	PBE	PBE+ vdW ^{surf}	PBE
	O–Au ₁	O–Au ₂	O–Au ₃	O–Au ₁	O–Au ₂	O–Au ₃				
1-propoxy on Au(111)	2.30	2.33	2.29	2.34	2.36	2.32	3.38	3.48	130.3	127.5
allyloxy on Au(111)	2.89	2.30	2.27	2.32	2.36	2.33	2.52	3.68	121.5	120.3
methallyloxy on Au(111)	2.89	2.30	2.27	2.32	2.36	2.32	2.72	3.63	121.6	119.5
1-propoxy on Au(110)	2.28	2.26	2.37	2.26	2.28	2.44	2.79	3.51	132.7	123.5
allyloxy on Au(110)	2.34	2.24	2.38	2.29	2.27	2.42	1.44	2.58	140.4	127.5
methallyloxy on Au(110)	2.34	2.23	2.38	2.29	2.27	2.40	1.48	2.31	140.5	128.5

^aStructural details of 1-propoxy, allyloxy, and methallyloxy, adsorbed on Au(110) and Au(111) surfaces calculated using PBE+vdW^{surf} and PBE methods. Refer to Figure 3 for the details of the employed notation. The angles (Au–O–C₁) were calculated from bond distances Au–O and O–C₁ using the cosine law; $\cos(\text{Au–O–C}_1) = [(\text{Au–O})^2 + (\text{O–C}_1)^2 - (\text{C–Au})^2] / 2 * (\text{Au–O}) * (\text{O–C}_1)$. Geometry details of all alkoxydes on both surfaces with and without vdW interactions can be found in Tables ST2 and ST3.

the calculated binding energies using water formation from OH as a reference reaction are essentially the same for *all* alkoxydes studied on both Au(111) and Au(110), 0.2 ± 0.02 eV (Table 2). Clearly, the calculations using PBE only are *not* even qualitatively consistent with experimental observations. Once the noncovalent interactions are included, the relative binding energies fully agree with the qualitative hierarchy obtained from experiment: $\text{OH}_{\text{ads}} < \text{CH}_3\text{O}_{\text{ads}} < \text{CH}_3\text{CH}_2\text{O}_{\text{ads}} < \text{CH}_3(\text{CH}_2)_2\text{O}_{\text{ads}} < (\text{CH}_3)_2\text{CH}_2\text{O}_{\text{ads}} < \text{H}_2\text{C}=\text{CHCH}_2\text{O}_{\text{ads}} < \text{H}_2\text{C}=\text{CH}(\text{CH}_3)\text{CH}_2\text{O}_{\text{ads}} < \text{C}_6\text{H}_5\text{CH}_2\text{O}_{\text{ads}}$ (Tables 1 and 2). The overall trend is the same on both Au(111) and Au(110); increasing the number of carbon moieties increases the vdW interactions between the alkoxyde and the surface. While it is possible that noncovalent interactions could play a role in determining the activation energy for displacement, the binding energies are a good proxy for the binding hierarchy since we have experimentally determined that it is determined by thermodynamics, not kinetics.

The vdW interactions increase on average by 0.10 eV per CH₂ group added for relatively short chains (up to 4 carbons) based on this work and on prior studies.⁵ This value is in good agreement with experimental determinations of the additive

effect of CH₂ in the binding energies of linear alkanes on Au(111) reported previously (0.06 ± 0.02 eV per carbon),²⁸ providing validation of the theoretical method.

The difference in the calculated binding energies of methoxy and ethoxy are similar on Au(110) and Au(111),⁵ consistent with the fact that the equilibrium constant for this pair is the same on both surfaces. The higher stability of methoxy/Au(110) when compared to methoxy/Au(111) stems from the bending of the CH₃ group toward the protrusions of the Au(110) surface induced by attractive vdW interactions (Figure 3a,b). This is consistent with the previous observation of increased vdW interactions of aromatic molecules with stepped metal surfaces.²⁹ We emphasize that quantitative comparison to equilibrium constants in experiment would require calculating free energies, hence both binding energies and the entropy of reaction would be required to calculate the equilibrium constant. Nevertheless, the insensitivity of the relative stability of alkoxydes to surface structure demonstrates that use of the vdW interactions is a robust factor for evaluating bond strengths for a homologous series of surface reaction intermediates.

The calculations show that carbon–carbon bond unsaturation and branching in the alkyl group also affects the stability of the alkoxides. Branching, as evaluated from the relative stability of 2-propoxide and 1-propoxide, has only a minimal effect in the calculations, 0.04–0.08 eV, which is close to the accuracy limits of the calculations (Table 2). Experiments on Au(110) clearly demonstrate that 2-propanol displaces 1-propoxide; however, the equilibrium constant was not determined in this case. The minimal difference in binding energy suggests that entropy may play a role in the experimental displacement hierarchy.

Carbon–carbon bond unsaturation increases the binding energy of the alkoxides more substantially. For example, the binding energy of allyloxy ($\text{H}_2\text{C}=\text{CHCH}_2\text{O}_{\text{ads}}$) is larger than that of 1-propoxy by 0.1 eV when vdW interactions are included in the calculations (Table 2). Addition of an extra methyl group in methylallyloxy leads to an additional 0.1 eV of stabilization relative to allyloxy, indicating that the effects of C=C unsaturation and the increased chain length are additive. The phenyl ring has the largest absolute stabilization due to vdW interactions, 0.64 eV on Au(111). This value is in excellent agreement with the experimentally determined value of the binding energy of benzene to Au(111)^{27,30} and in reasonable agreement with previous DFT calculations thereof (Table 2).²⁶ The effect of the phenyl ring includes both carbon–carbon unsaturation and interaction of additional carbon groups.

The inclusion of vdW interactions alters the structure of the adsorbed species, which may, in turn, affect the magnitude of the effect of C=C bonds (Tables 3 and Tables ST2 and ST3). For example, the Au–O–C₁ bond angle of 1-propoxy increases when vdW interactions are included, from 127.5° to 130.3° on Au(111) and from 123.5° to 132.7° on Au(110), such that the alkyl chain is tilted more toward the surface (Figure 4). This tilting results in a decrease in the distance between the Au and the terminal carbon (C₃) from 3.48 Å (PBE only) to 3.38 Å (PBE+vdW^{surf}) on Au(111) and from 3.51 to 2.79 Å on Au(110) (PBE+vdW^{surf}) on Au(110) and from 3.51 to 2.79 Å on Au(110) (PBE+vdW^{surf}) on Au(110).

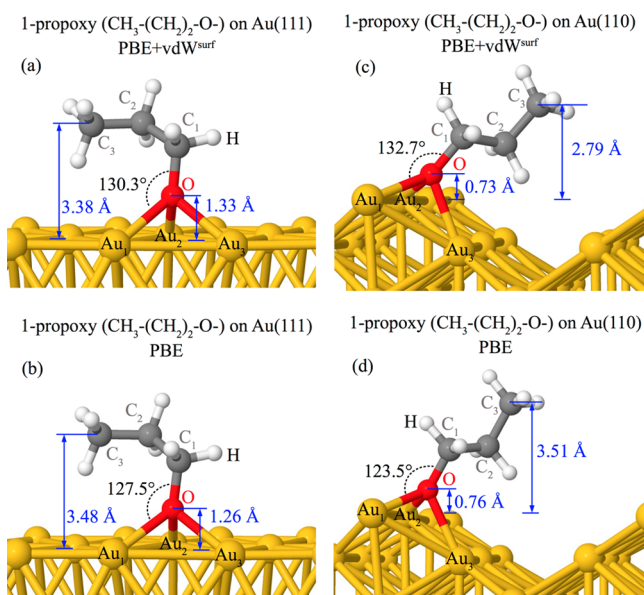


Figure 4. Optimized structures. 1-Propoxy on the Au(111) (left) and Au(110) (right) surfaces, calculated with (top) and without (bottom) vdW interactions. The key structural parameters are shown in the figure.

Au(110), reflecting the attraction between the hydrocarbon tail and the Au surface. The differences in bond distances presumably reflect a balance between the covalent O–Au bond and the noncovalent interaction of the alkyl group with the underlying surface.

Similar structural changes occur when vdW interactions are included for the other alkoxides bound to Au. All relaxed structures with or without vdW and their relevant structural parameters for the adsorbed intermediates on Au(111) and Au(110) can be found in Tables ST2 and ST3. The Au–O–C₁ bond angle generally increases, and the chain of the intermediate is tilted toward the surface upon inclusion of the vdW interactions in the calculations (Figures S4 and S5). Benchmark studies of the FHI-aims and VASP codes on methoxy adsorption on Au(111) showed that the two codes used in this study produce quantitatively similar reaction energies (Table ST3). The inclusion of vdW interaction in both codes optimizes the stable geometries adsorbed on Au surface.

DISCUSSION

The structures calculated for the various alkoxides reflect the interaction of the alkyl groups with the surface for both Au(111) and Au(110) (Figures 3, 4, S4, and S5 and Tables ST2 and ST3). The vdW interactions alter the structure of the adsorbed species for all intermediates studied. The inclusion of vdW interactions generally leads to a tilting of the alkyl chain toward the surface on both Au(111) and Au(110). Allyloxy, which contains a C=C bond in the alkyl chain, is almost parallel to the Au surfaces as shown in Figure 3c,d. Such effects of bringing the adsorbates closer to the surface by vdW interactions can be also observed in benzyl alkoxy, where the carbon rings lie again parallel to the surfaces. This tilting, for example, results in an overall decrease of the distance between Au surface and C3 in the methylallyloxy chain, by ~0.8 Å on both Au surfaces (Tables ST2 and ST3), when the vdW interactions are included. Similar effects have been observed previously by NEXAFS studies of unsaturated alcohols on Ag(110).³¹ It has been shown that the orientation of the π orbital in allyl alcohol and allyloxy on the Ag(110) single crystal clearly indicates bonding interactions between the double bond and the surface, to produce ordering. The azimuthal ordering of allyloxy leads to a parallel orientation of the surface intermediate, being consistent to the observations of the present study for allyloxy on Au(110).

It is noteworthy that the reaction energy hierarchy of seven different alkoxides (Table 2) and that the equilibrium constants for competitive binding of methoxy and ethoxy (Figure 2) are the same on Au(111) and Au(110), indicating a lack of structure sensitivity for alkoxide binding to these Au surfaces. The absence of a strong structure sensitivity is further demonstrated by the correspondence in reaction selectivity for the oxidative coupling of dissimilar alcohols on Au(111) and Au(110) and on nanoporous Au catalysts (Figure 1). Even so, there is a precedent for strong structure sensitivity for other classes of reactions (C–C and C–N coupling) catalyzed by shape-controlled nanostructures.^{32,33} For example, shorter Au nanorods with a predominance of (111) facets are much more selective for Sonogashira C–C cross coupling,³² and Au nanoplatelets also with a predominance of (111) facets have substantially higher activity for C–C and C–N coupling.³³ Both of the investigations of nanomaterials^{32,33} were performed in solution and involved aromatic molecules. As demonstrated herein for the case of benzylalkoxy, when vdW interactions are

included, the binding of the phenyl ring with the Au is especially strong, and there is a significant difference in binding energy (0.1 eV) for Au(111) vs Au(110) (Table 2). Further investigation is necessary to determine if the structure sensitivity is specific to aromatic rings or if it is related to the different binding modes for the intermediates in these different classes of reaction.

Despite the lack of structure sensitivity measured experimentally, there are several differences in detail in bonding that are evident from analysis of the calculations. First, the vdW-induced stabilization for methoxy, ethoxy, 1-propoxy, 2-propoxy, and benzyl alkoxy is larger on Au(110) surface than on Au(111). This finding cannot be explained by the packing density of the surface and is attributed to the ability of molecules to tilt toward the protrusions of the Au(110) surface, thereby optimizing the noncovalent vdW attraction to the surface. Second, the inclusion of vdW interactions typically has no effect on changing the O–Au adsorption site, except for allyloxy and methallyloxy on Au(111). In these cases, the vdW attraction of the unsaturated π system is optimized by displacing the O–Au bond toward the bridge site, elongating the O–Au1 bond (Figure 3c,d). Therefore, the vdW interactions play a qualitative role for allyloxy and methallyloxy on Au(111), changing the nature of the O–Au bond. This fact is also confirmed by an increase of 0.24 eV in the PBE reaction energy between PBE-optimized and PBE+vdW^{surf}-optimized structures, which is more than compensated by vdW interactions. Finally, noncovalent interactions also have a slight effect on the electronic properties of alkoxides on Au(111), increasing the band gap from 0.01 to 0.02 eV. Another difference between Au(110) and Au(111) surfaces is the amount of charge transfer between alkoxides and the surface. While the computed Hirshfeld charge transfer is negligible for Au(111), it amounts to 0.2 electrons for Au(110).

Here we have focused our studies on alcohol intermediates binding strength on Au, which is relevant to selective oxidative reactions. While the effect of vdW interactions is clearly important for predicting the binding strength of various intermediates to gold, the intermediates are bound relatively weakly to Au; thus the vdW interactions will naturally account for a large percentage of the binding energy. A key question we are pursuing is to what extent will noncovalent interactions affect relative stability of bonding on other transition-metal surfaces and catalysts. Stronger binding of the primary functional group to late-transition metals such as Ni or Pd could lead to either stronger or weaker vdW interactions with the surface. On the one hand, the stronger bonding would bring the adsorbed molecule closer to the surface; on the other, the stronger bonding may render structural rearrangement that leads to substantial noncovalent interactions between the surface and the adsorbate that will be more energetically costly. If the relative contribution of the vdW interactions is different across the periodic table, new scaling relationships that include these subtleties will be required.

The same principles about the binding strength of reaction intermediates also relate to other types of reactions and catalyst surfaces. Adsorbed intermediates can lead to side products, such as adsorbed carboxylates which can also compete for binding sites.^{34,35} Strongly bound species, such as carboxylates, may inhibit reaction by blocking formation of other key reactive intermediates.^{36–38}

The qualitative trends in binding energy for alkoxides also correlate with the gas-phase Brønsted acidity on these Au

surfaces as well as for Ag(110)³⁹ and for anatase TiO₂,⁴⁰ providing a simple scale that can be used to predict relative binding efficacy. Both the gas-phase acidity and the magnitude of vdW interactions scale with polarizability, providing a rationale for the two different correlations. The correlation with gas-phase acidity and binding of alkoxides to TiO₂ had to be scaled, which is consistent with the expectation that the bonding to oxides will be different than to the coinage metals.

The present work adds a critical dimension to the current framework of reactivity on gold catalysts, by addressing the effects of chain branching configuration, C=C double bonds, and structure sensitivity on the relative binding efficacy of key reactive intermediates in the oxidative alcohols. We have explicitly demonstrated the key role of vdW interactions on reaction selectivity, providing a clear basis for predicting and understanding how to control selectivity in complex environments.

CONCLUSIONS

In summary, the selectivity of a wide range of heterogeneous chemical reactions is affected by the relative stability of surface intermediates on the catalyst surface, affecting the sustainability of the chemical production. We demonstrate that noncovalent vdW interactions determine the surface stability of alcohol's reactive intermediates and thus the selectivity of oxidation reactions on Au surfaces, by modulating the competition of key reactants toward surface oxygen. The key factors that clearly affect the surface stability of intermediates on Au are the branching configuration of the alkyl group, the unsaturated C=C bonds, and the aromatic rings in certain organic compounds. The contribution due to the long-range vdW interaction is found to be ~ 0.1 eV per carbon, the unsaturated C=C bond adds an additional ~ 0.1 eV in the vdW contribution, and a similar increase in the vdW contribution is added when branching configuration of the alkoxy is present. The intermediate binding on the surface does not appear to be sensitive to the structure of the catalyst's surface. By defining the relative stability of reaction intermediates, a general approach toward the optimization of various reaction selectivities can be established, increasing the sustainability of various heterogeneous catalytic procedures.

ASSOCIATED CONTENT

Supporting Information

The Supporting Information is available free of charge on the ACS Publications website at DOI: 10.1021/jacs.6b09450.

Experimental procedure, competition between surface intermediates, experimental hierarchy, signature products and desorption temperatures on Au(110) and Au(111) surfaces, control of dosing the reactants, isolation of X_{ads}, temperature-programmed reaction spectra for the oxidation reaction of alcohols on Au(110), displacement experimental results for the stability hierarchy on Au(110), 2-propanol vs 1-propanol displacement reaction on Au(110) at 180 K, constants used in the quantitative mass spectrometry analysis, temperature-programmed reaction spectra for the 85:15 methanol/ethanol mixture on O/Au(110) interface, PBE+vdW^{surf} optimized geometries of the systems that were studied, optimized geometry of methoxy adsorbed on Au(111) studied using PBE+vdW^{surf} method, optimized structural details of the systems adsorbed on Au(111), optimized

structural details of the systems adsorbed on Au(110), benchmark studies of the codes of FHI-aims and VASP, reaction energies of methoxy adsorbed on Au(111) computed using FHI-aims and VASP (PDF)

AUTHOR INFORMATION

Corresponding Author

*friend@fas.harvard.edu

Present Address

^{||}Department of Chemical Engineering, Swearingen Engineering Center, University of South Carolina, Columbia, SC 29208, United States

Notes

The authors declare no competing financial interest.

ACKNOWLEDGMENTS

This work was supported as part of the Integrated Mesoscale Architectures for Sustainable Catalysis, an Energy Frontier Research Center funded by the U.S. Department of Energy, Office of Science, Basic Energy Sciences, grant no. DE-SC0012573. This research used resources of the Oak Ridge Leadership Computing Facility (OLCF) and the National Energy Research Scientific Computing Center (NERSC) of the U.S. Department of Energy.

REFERENCES

- (1) Wang, S.; Petzold, V.; Tripkovic, V.; Kleis, J.; Howalt, J. G.; Iason, E. S.; Fernandez, M.; Hvolbæk, B.; Jones, G.; Toftelund, A.; Falsig, H.; Bjorketun, M.; Studt, F.; Abild-Pedersen, F.; Rossmeisl, J.; Nørskov, J. K.; Bligaard, T. *Phys. Chem. Chem. Phys.* **2011**, *13*, 20760–20765.
- (2) Abild-Pedersen, F.; Greeley, J.; J. Greeley, F. S.; Rossmeisl, J.; Munter, T. R.; Moses, P. G.; Skúlason, E.; Bligaard, T.; Nørskov, J. K. *Phys. Rev. Lett.* **2007**, *99* (1–6), 016105.
- (3) Nørskov, J. K.; Abild-Pedersen, F.; Studt, F.; Bligaard, T. *Proc. Natl. Acad. Sci. U. S. A.* **2011**, *108* (3), 937–943.
- (4) Jones, G.; Jakobsen, J. G.; Shim, S. S.; Kleis, J.; Andersson, M. P.; Rossmeisl, J.; Abild-Pedersen, F.; Bligaard, T.; Helveg, S.; Hinnemann, B.; Rostrup-Nielsen, J. R.; Chorkendorff, I.; Sehested, J.; Nørskov, J. K. *J. Catal.* **2008**, *259* (1), 147–160.
- (5) Rodríguez-Reyes, J. C. F.; Siler, C. G. F.; Liu, W.; Tkatchenko, A.; Friend, C. M.; Madix, R. J. *J. Am. Chem. Soc.* **2014**, *136* (38), 13333–13340.
- (6) Xu, B.; Madix, R. J.; Friend, C. M. *J. Am. Chem. Soc.* **2010**, *132* (46), 16571–16580.
- (7) Xu, B.; Liu, X.; Haubrich, J.; Friend, C. M. *Nat. Chem.* **2010**, *2*, 61–65.
- (8) Wang, B.; Sun, W.; Zhu, J.; Ran, W.; Chen, S. *Ind. Eng. Chem. Res.* **2012**, *51* (46), 15004–15010.
- (9) Suzuki, K.; Yamaguchi, T.; Matsushita, K.; Iitsuka, C.; Miura, J.; Akaogi, T.; Ishida, H. *ACS Catal.* **2013**, *3* (8), 1845–1849.
- (10) Wang, L.-C.; Stowers, K. J.; Zugic, B.; Personick, M. L.; Biener, M. M.; Biener, J.; Friend, C. M.; Madix, R. J. *J. Catal.* **2015**, *329*, 78–86.
- (11) Zugic, B.; Karakalos, S.; Stowers, K. J.; Biener, M. M.; Biener, J.; Madix, R. J.; Friend, C. M. *ACS Catal.* **2016**, *6*, 1833–1839.
- (12) Saliba, N.; Parker, D. H.; Koel, B. E. *Surf. Sci.* **1998**, *410* (2–3), 270.
- (13) Gottfried, J. M. Ph.D. Dissertation, Freien Universität, Berlin, 2003.
- (14) Rodríguez-Reyes, J. C. F.; Friend, C. M.; Madix, R. J. *Surf. Sci.* **2012**, *606* (15–16), 1129–1134.
- (15) Madix, R. J. *Surf. Sci.* **1994**, *299–300*, 785–797.
- (16) Blum, V.; Gehrke, R.; Hanke, F.; Havu, P.; Havu, V.; Ren, X.; Reuter, K.; Scheffler, M. *Comput. Phys. Commun.* **2009**, *180* (11), 2175–2196.

(17) Kresse, G.; Furthmüller, J. *Phys. Rev. B: Condens. Matter Mater. Phys.* **1996**, *54* (16), 11169–11186.

(18) Lejaeghere, K.; Bihlmayer, G.; Björkman, T.; Blaha, P.; Blügel, S.; Blum, V.; Caliste, D.; Castelli, I. E.; Clark, S. J.; Corso, A. D.; Gironcoli, S. d.; Deutsch, T.; Dewhurst, J. K.; Marco, I. D.; Draxl, C.; Dulak, M.; Eriksson, O.; Flores-Livas, J. A.; Garrity, K. F.; Genovese, L.; Giannozzi, P.; Giantomassi, M.; Goedecker, S.; Gonze, X.; Grånäs, O.; Gross, E. K. U.; Gulans, A.; Gygi, F.; Hamann, D. R.; Hasnip, P. J.; Holzwarth, N. A. W.; Iuşan, D.; Jochym, D. B.; Jollet, F.; Jones, D.; Kresse, G.; Koepnick, K.; Küçükbenli, E.; Kvashnin, Y. O.; Loch, I. L. M.; Lubeck, S.; Marsman, M.; Marzari, N.; Nitzsche, U.; Nordström, L.; Ozaki, T.; Paulatto, L.; Pickard, C. J.; Poelmans, W.; Probert, M. I. J.; Refson, K.; Richter, M.; Rignanese, G.-M.; Saha, S.; Scheffler, M.; Schlipf, M.; Schwarz, K.; Sharma, S.; Tavazza, F.; Thunström, P.; Tkatchenko, A.; Torrent, M.; Vanderbilt, D.; Setten, M. J. v.; Speybroeck, V. V.; Wills, J. M.; Yates, J. R.; Zhang, G.-X.; Cottenier, S. *Science* **2016**, *351*, 6280.

(19) Tkatchenko, A.; Scheffler, M. *Phys. Rev. Lett.* **2009**, *102* (7), 073005.

(20) Ruiz, V. G.; Lui, W.; Wei Liu, E. Z.; Scheffler, M.; Tkatchenko, A. *Phys. Rev. Lett.* **2012**, *108* (14), 146103.

(21) Lifshitz, E. M. *Sov. Phys. - J. Exp. Theor. Phys.* **1956**, *2* (1), 73–83.

(22) van Lenthe, E.; Baerends, E. J.; Snijders, J. G. *J. Chem. Phys.* **1994**, *101*, 9783–9792.

(23) Kresse, G.; Joubert, D. *Phys. Rev. B: Condens. Matter Mater. Phys.* **1999**, *59* (3), 1758–1775.

(24) Perdew, J. P.; Burke, K.; Ernzerhof, M. *Phys. Rev. Lett.* **1996**, *77* (18), 3865.

(25) Methfessel, M.; Paxton, A. T. *Phys. Rev. B: Condens. Matter Mater. Phys.* **1989**, *40* (6), 3616–3621.

(26) Wellendorff, J.; Kelkkanen, A.; Mortensen, J. J.; Lundqvist, B. I.; Bligaard, T. *Top. Catal.* **2010**, *53* (5), 378–383.

(27) Syomin, D.; Kim, J.; Koel, B. E.; Ellison, G. B. *J. Phys. Chem. B* **2001**, *105* (35), 8387–8394.

(28) Wetterer, S. M.; Lavrich, D. J.; Cummings, T.; Bernasek, S. L.; Scales, G. J. *Phys. Chem. B* **1998**, *102* (46), 9266–9275.

(29) Camarillo-Cisneros, J.; Liu, W.; Tkatchenko, A. *Phys. Rev. Lett.* **2015**, *115* (8), 086101.

(30) Liu, W.; Maaß, F.; Willenbockel, M.; Bronner, C.; Schulze, M.; Soubatch, S.; Tautz, F. S.; Tegeder, P.; Tkatchenko, A. *Phys. Rev. Lett.* **2015**, *115*, 036104.

(31) Solomon, J. L.; Madix, R. J.; Stöhr, J. *J. Chem. Phys.* **1988**, *89* (8), 5316.

(32) Lin, J.; Abroshan, H.; Liu, C.; Zhu, M.; Li, G.; Haruta, M. *J. Catal.* **2015**, *330*, 354–361.

(33) Primo, A.; Esteve-Adell, I.; Coman, S. N.; Candu, N.; Parvulescu, V. I.; Garcia, H. *Angew. Chem.* **2016**, *128*, 617–622.

(34) Liu, X.; Xu, B.; Haubrich, J.; Madix, R. J.; Friend, C. M. *J. Am. Chem. Soc.* **2009**, *131* (16), 5757–5759.

(35) Barteau, M.; Bowker, M.; Madix, R. J. *J. Catal.* **1981**, *67*, 118.

(36) Hao, Y.; Mihaylov, M.; Ivanova, E.; Hadjiivanov, K.; Knozinger, H.; Gates, B. C. *J. Catal.* **2009**, *261* (25), 137–149.

(37) Schubert, M. M.; Venugopal, A.; Kahlich, M. J.; Plzak, V.; Behm, R. J. *J. Catal.* **2004**, *222* (1), 32–40.

(38) Daté, M.; Okumura, M.; Tsubota, S.; Haruta, M. *Angew. Chem., Int. Ed.* **2004**, *43*, 2129–2132.

(39) Barteau, M. A.; Madix, R. J. *Surf. Sci.* **1982**, *120* (2), 262–272.

(40) Silbaugh, T. L.; Boaventura, J. S.; Barteau, M. A. *Surf. Sci.* **2016**, *650*, 64–70.